



# International Operational Modal Analysis Conference

20 - 23 May 2025 | Rennes, France

## Finite Element Model Updating of a Small-Scale Wind Turbine Blade Using Strain-Based Pull-and-Release Test Data

*Silvia Vettori*<sup>1</sup>, *André Tavares*<sup>1,2</sup>, *Mirco Giorgi*<sup>3</sup>, *Emilio Di Lorenzo*<sup>1</sup>, and *Giuliano Coppotelli*<sup>3</sup>

<sup>1</sup> Siemens Digital Industries Software, Interleuvenlaan 68, 3000, Leuven, Belgium

<sup>2</sup> KU Leuven, Department of Mechanical Engineering, Celestijnenlaan 300, Leuven, 3001, Belgium

<sup>3</sup> University of Rome "La Sapienza", Faculty of Civil and Industrial Engineering, Department of Mechanical and Aerospace Engineering, via Eudossiana 18, 00184 Rome, Italy

### ABSTRACT

In view of the increasing industrial need of reducing Wind Turbines (WTs) operational costs, improved Structural Health Monitoring (SHM) strategies are nowadays exploited and further boosted through innovative digitalization processes. The aim of these schemes consists in tracking and supporting blades status assessment not only in the field, but also from conceptualization, through certification tests, all the way to operation and end-of-life. Extensive testing is usually performed on blades prior to installation. Although more attention is usually placed on static and fatigue tests, dynamic tests are also adopted for identifying basic dynamic properties, essential for the structural integrity of the entire WT. The modal parameters obtained from dynamic tests, such as natural frequencies and mode shapes, are often used to update structural models and create test-validated digital twins. While effective, this conventional approach to model updating is inherently global, thus potentially introducing inaccuracies in capturing localized material behaviors. Additionally, this methodology predominantly relies on acceleration measurements, thereby excluding static model validation, which requires separate analysis. To address these limitations, this study proposes the use of strain measurements acquired via fiber-optic sensors, to update the Finite Element Model (FEM) of a small-scale Glass Fiber Reinforced Plastic (GFRP) wind turbine blade. This strain data is integrated into an optimization framework employing local criteria to assess model accuracy.

*Keywords: wind turbine blade; model updating; strain sensors; fiber optics; pull and release test*

### 1. INTRODUCTION

Wind Turbine (WT) blades are complex, flexible structures subjected to dynamic loads from wind, grav-

ity, and operational conditions. Ensuring their structural integrity and performance requires accurate Finite Element Models (FEMs) [1] that capture their real-world behavior. However, uncertainties in material properties, manufacturing defects, and environmental effects often lead to discrepancies between numerical predictions and actual structural responses. Model updating techniques help refine FEMs by incorporating experimental data, thereby improving their predictive accuracy. Reference experimental data is often represented by global modal parameters extracted via acceleration-based Experimental or Operational Modal Analysis [2, 3]. However, with the advancement of modal identification techniques, there is a growing interest in deploying strain sensors for vibration testing [4, 5]. Traditionally, resistive strain gauges have been widely used for this purpose. Nevertheless, the emergence of fiber-optic sensing has introduced a range of advantages that make it a superior alternative in many applications [6], including wind turbine blades testing and monitoring [7]. Key benefits of fiber-optic sensors are their insensitivity to electromagnetic interferences, their small dimensions and lightweight nature and their compact size, which allows for easy integration into structures without adding significant weight. Specifically, their minimal footprint makes them particularly suitable for embedding into composite materials, leading to the development of smart structures, e.g., wind turbine blades, that can self-monitor their integrity over time.

This paper explores the role of Fiber Bragg Grating (FBG) sensors in improving wind turbine blade FEMs through model updating techniques. Specifically, the hereby presented case study deals with testing and model updating of a small-scale wind turbine blade. The test campaign is first presented, along with the experimental results and the modal parameters extracted via Operational Modal Analysis (OMA). The measured strain responses are adopted as reference in both a single and a multi-objective optimization framework aimed at updating the FEM material parameters with the purpose of minimizing model deviations with respect to the reference data sets. The two approaches are evaluated for their performance in providing: i) the lowest error between numerical and experimental natural frequencies, ii) the highest correlation between measured and simulated strain responses.

## 2. SMALL-SCALE WIND TURBINE BLADE OMA

The hereby analyzed experimental case study deals with testing of the small-scale composite WT blade in Figure 1 (left). The scaled blade has been designed and manufactured by DTU Wind and Energy Systems via a typical resin infusion process with glass fibers and Balsa wood core. The small composite blade under study features two shear webs, i.e., two reinforcements spanning  $3/4$  of the blade length, and an aluminum insert at the root. The latter has been added for allowing the blade attachment to a support or to a scaled WT hub through a bolted connection.

### 2.1. Measurement campaign

Figure 1 (left) illustrates the scaled blade setup adopted during the test carried out at Siemens Industry Software (SISW) in cooperation with Sentea. During the tests, the blade root has been clamped via a 6-bolt connection between the aluminum insert and a steel plate anchored to a testbed. The blade suction surface has been equipped with two arrays of 5 FBG sensors each, whose locations are indicated in Figure 1 (left). Vibration measurements have been collected with the Sentea DM-4120 FBG interrogator. Excitation has been provided by pulling the blade tip and releasing it, to generate free oscillations. The strain responses have been acquired and then exported to Simcenter<sup>TM</sup> Testlab (Figure 1 (right)). Here, the 10 recorded strain signals have been processed via Simcenter<sup>TM</sup> Testlab Operational PolyMAX to determine the scaled blade modal parameters. The resulting stabilization diagram is provided in Figure 2. It is worth noting that the reported Crosspowers sum is derived from a filtering and windowing scheme designed to produce cleaner stabilization diagrams. As a result, only a single predominant peak appears in the diagram. However, the algorithm successfully identifies the first five modes of the blade. Table 1 lists the identified natural frequencies and damping ratios, along with a description of the mode shapes. The classification of the reported modes was performed through visual inspection of the strain mode shapes, with validation supported by the FEM described in Section 3.1..

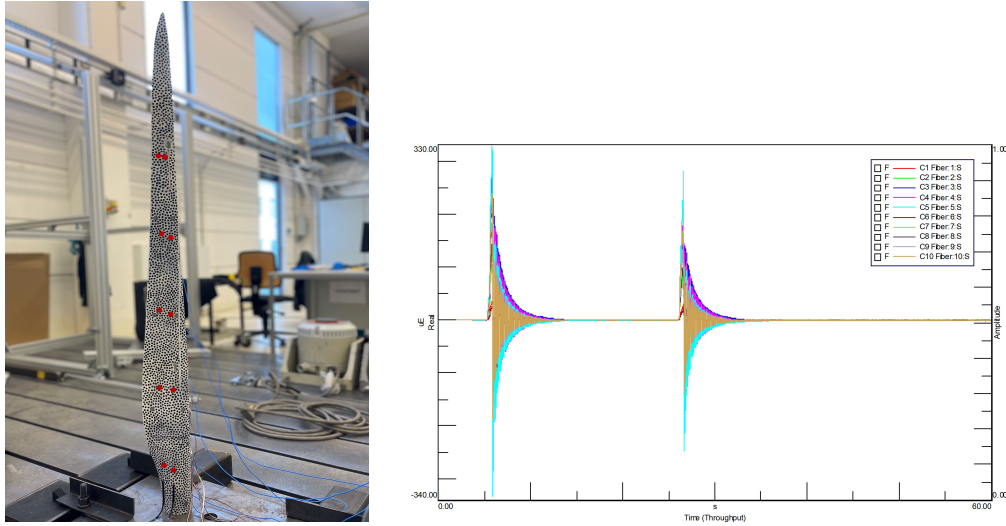


**Figure 1:** Small-scale WT blade test - setup and FBGs locations (left), recorded strain signals (right)

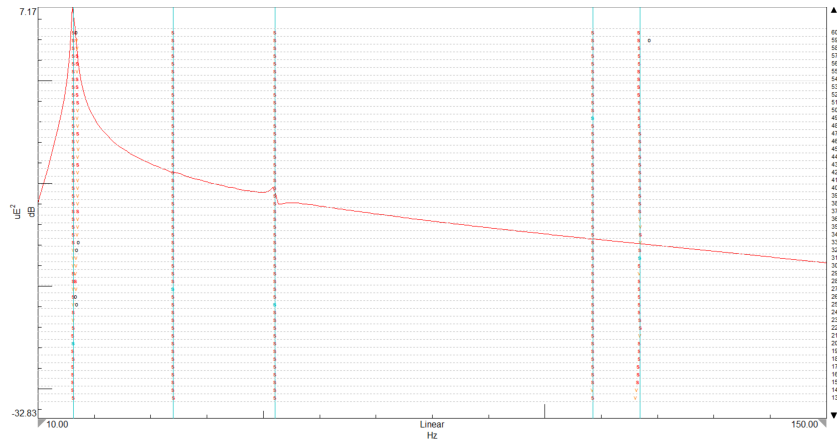


**Figure 2:** Small-scale WT blade test - Simcenter <sup>TM</sup> Testlab Operational PolyMAX

Modes	Frequency [Hz]	Damping [%]	Mode type
1	16.26	0.83	First flap-wise bending
2	34.06	0.97	First edge-wise bending
3	52.07	0.80	Second flap-wise bending
4	108.56	0.85	Second edge-wise bending
5	116.27	1.45	Third flap-wise bending

**Table 1:** Small-scale WT blade experimental modal parameters in clamped-free conditions

### 3. SMALL-SCALE WIND TURBINE BLADE MODEL UPDATE

#### 3.1. Finite Element Model

The FEM of the small-scale composite blade, offered in 3 (left), has been developed by DTU Wind and Energy Systems via the in-house Blade Modeling Tool and solved in Simcenter<sup>TM</sup> Nastran. It is composed of 92423 CHEXA elements (8 nodes) with associated solid composite property (PCOMPs). The FEM features 6 materials in total: Aluminum, Glue (isotropic materials), Balsa wood, Uniaxial, Biaxial and UD90 fabrics (orthotropic materials). To reproduce the test Boundary Conditions (BCs), the constraints shown in Figure 3 (center) have been defined at the blade FEM root by means of 6 RBE2 (Rigid Body Elements) with fixed independent nodes. Additionally, as indicated in Figure 3 (right), a

RBE3 has been defined at the tip to model the load application area adopted during the test.

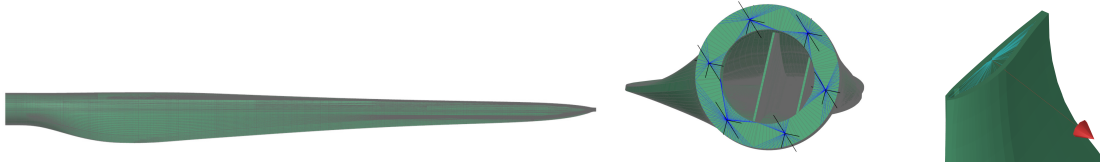


**Figure 3:** Small-scale WT blade FEM (left), FEM BCs (center) and FEM load application point (right)

### 3.2. Model update

The proposed model updating strategy involves using transient simulations to generate synthetic data to be compared against the strain responses obtained via the FBGs during the pull and release test. To produce accurate forward-simulated data, a force has been defined at the blade FEM tip (Figure 3), in the same direction of the physically applied force. To virtually reproduce the test, the time history of the load has been defined as a linear ramp from  $F = 0$  at  $t = 0$  to  $F = \tilde{F}$  at  $t = \tilde{t}$ , with  $t = \tilde{t}$  being the blade release instant. To define the equivalent load amplitude, a MATLAB <sup>TM</sup>-based routine has been constructed to interact with the inputs and outputs of Simcenter <sup>TM</sup> Nastran SOL 101 (static solution). This allowed to implement an algorithm aimed at minimizing the square of the strain signal energy. This approach has identified a force at the release instant  $\tilde{F}$  equal to 3.254 N. The resulting load time history has been used to generate transient simulation data via Simcenter <sup>TM</sup> Nastran SOL 112 (Modal Transient Response Analysis).

The model updating workflows developed in this work aim at identifying the most appropriate combination of material properties which guarantees the highest correlation between the simulated and the experimentally acquired strain responses. The updating strategy has been implemented in a MATLAB <sup>TM</sup>-based environment, where the optimization variables, i.e., the material properties, are sampled in the user-defined ranges reported in Table 2. At each iteration, the routine creates a Simcenter <sup>TM</sup> Nastran source file and interacts with the solver to launch and extract the simulation results. The objective function can be then minimized (or maximized) to obtain the best material parameters combination. To reduce the computational burden, only in-plane stiffness material properties ( $E_1$ ,  $E_2$ ,  $\nu_{12}$ ) and  $\rho$  are used as design variables for orthotropic materials. Indeed, out-of-plane effects have lower influence on simulated deformations of composite materials due to their layered structure. Additionally, Glue has been excluded from the optimization due to its minor effect. Material properties not included in the optimization variables set were assigned their baseline values, except for the shear moduli which are automatically changed during the optimization process according to materials constitutive laws.

Two different approaches have been adopted to solve the optimization problem: a single-objective Surrogate Optimization (SO) and a multi-objective Genetic Optimization (GO).

**Single-objective Surrogate Optimization** The SO [8, 9] is an advanced technique within the field of global optimization which leverages surrogate models—approximate representations of the objective function to efficiently explore the solution space and identify optimal solutions with reduced computational overhead. The SO operates by iteratively constructing surrogate models and searching for minima based on these models, thereby balancing exploration and exploitation to converge towards the global optimum. For the application proposed in this paper, the minimum number of random points used to build the surrogate function has been set to 500, while the batch update interval has been set to 1 so that the surrogate is updated at each evaluation. The minimum sample distance has been set to 0.001.

The objective function employed for the SO is the Frequency Response Indicator (FRI):

$$FRI = 1 - \frac{1}{N_{ch.}} \sum_{i=1}^{N_{ch.}} FRAC_{i,i} \quad (1)$$

Material	Property	Central Value	Lower Bound %	Upper Bound %
BIAX	$E_1$ [kPa]	1.45E+07	10	10
	$E_2$ kPa]	1.45E+07	10	10
	$\nu_{12}$ [ ]	0.533	10	10
	$\rho$ [kg/m <sup>3</sup> ]	2.00E-06	10	10
ALU	$E$ [kPa]	7.00E+07	15	15
	$\nu$ [ ]	0.3	10	10
	$\rho$ [kg/m <sup>3</sup> ]	2.70E-06	10	10
UNIAX	$E_1$ [kPa]	4.11E+07	20	20
	$E_2$ [kPa]	1.22E+07	20	20
	$\nu_{12}$ [ ]	0.275	20	20
	$\rho$ [kg/m <sup>3</sup> ]	1.98E-06	20	20
BALSA	$E_1$ [kPa]	2.35E+06	20	20
	$E_2$ [kPa]	2.35E+06	40	5
	$\nu_{12}$ [ ]	0.400	20	20
	$\rho$ [kg/m <sup>3</sup> ]	1.45E-06	20	20
UD90	$E_1$ [kPa]	1.22E+07	20	20
	$E_2$ kPa]	4.11E+07	20	20
	$\nu_{12}$ [ ]	0.0810	20	20
	$\rho$ [kg/m <sup>3</sup> ]	2.60E-06	20	20

**Table 2:** Small-scale WT blade FE model update: design variables initial values and range bounds

where the Frequency Response Assurance Criterion (FRAC) [10] is computed between the regularized Power Spectral Density (PSD) of the  $i^{th}$  channel of the numerical and experimental data sets. The PSD regularization process has been applied in this context to allow for equivalent weighting of the different modes within the overall optimization function. Indeed, the first flap-wise bending is predominant in signals recorded (or simulated) during a pull and release test. The regularization, which consisted in splitting the signal into different segments subjected to different band-pass windows, allowed to obtain experimental and numerical PSDs with peaks of comparable amplitude at the analyzed natural frequencies.

**Multi-objective Genetic Optimization** The presence of less excited modes during the pull and release test has been also tackled via an alternative approach which foresees the use of a variant of the Non-Dominated Sorting Genetic Algorithm II (NSGA-II) [11, 12]. A Genetic Algorithm (GA) is a method for solving both constrained and unconstrained optimization problems based on a natural selection process that mimics biological evolution. The adoption of this method allowed to solve a multi-objective optimization for two specific functions: the Time Response Indicator (TRI) and the global frequency error. The TRI is calculated as:

$$TRI = 1 - \frac{1}{N_{ch.}} \sum_{i=1}^{N_{ch.}} TRAC_{i,i} \quad (2)$$

where the TRAC (Time Response Assurance Criterion) [10] is computed between the simulated strain time history of each channel and the respective experimental measurement. The second objective function is computed as:

$$F_{err} = \frac{100}{N_{modes}} \sum_{i=1}^{N_{modes}} \frac{|f_i - \tilde{f}_i|}{\tilde{f}_i} \quad (3)$$

where  $N_{modes}$  is the number of modes in the frequency range of interest,  $f_i$  is the  $i^{th}$  numerical natural frequency and  $\tilde{f}_i$  the respective experimental one. The combination of these two objectives allowed to: i) use time signals in the optimization without the need of computing the PSDs, thus avoiding introducing uncertainties due to the chosen frequency spectra calculation method, ii) equivalently weight the modes in the frequency range of interest, i.e., avoiding the first mode taking over the optimization.

**Model updating results** Figure 4 shows the optimal design variables selected by both the SO and the GO in the user-defined ranges. The resulting updated FEMs are evaluated in this paper by means of Figure 5 and Figure 6, which respectively illustrate a comparison of the strain time histories and PSDs simulated via the updated (via both the SO and the GO) and baseline models against the reference test data. Additionally, Table 3 reports on the numerical natural frequencies of the baseline and updated models and compares them with the reference test natural frequencies. From the comparison of strain time histories, it can be concluded that both the SO and the GO guarantee a significant improvement of the correlation between the model and the reference test data in terms of response amplitude and phase. Indeed, Table 3 and Figure 6 confirm that both the approaches allow to well match the predominant first mode. However, the GO yields slightly lower errors for modes 1 and 2, while the SO more accurately tracks modes 3, 4, and 5. Overall, the two algorithms achieve comparable results, with the GO guaranteeing a lower percentage variation of the design variables with respect to their baseline values.

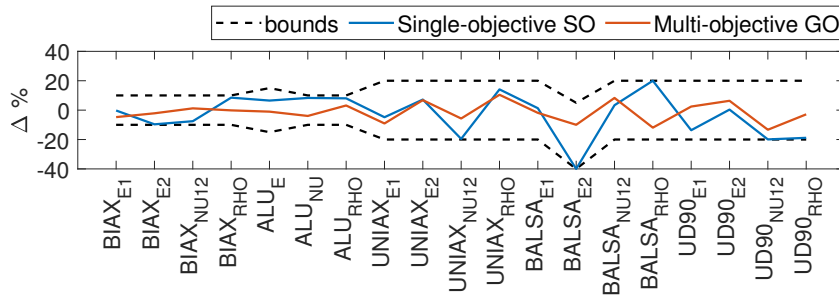


**Figure 4:** Small-scale WT blade FE model update: design variables updated values

Mode	Test Freqs. [Hz]	Baseline Freq.[Hz]	Updated Freq. - SO[Hz]	Updated Freq. - GO[Hz]
1	16.26	16.71	16.19	16.23
2	34.06	35.29	34.01	34.03
3	52.07	55.75	52.05	52.42
4	108.56	117.63	109.20	110.15
5	116.27	131.13	121.62	122.75

**Table 3:** Small-scale WT blade reference, baseline and updated numerical natural frequencies

#### 4. CONCLUSIONS

This work reports on the development and validation of a model updating framework for a small-scale composite blade by using reference data acquired via fiber-optic sensors. The scaled blade, equipped with two FBG arrays, has been tested in clamped-free conditions via a pull and release excitation. The acquired strain data has been used: i) for strain-based OMA, ii) as reference for the blade model update. For the latter, a MATLAB<sup>TM</sup>-based framework has been implemented to interact with Simcenter<sup>TM</sup> Nastran Modal Transient Response Analysis and select the optimal FEM material properties to optimize the selected objective functions through a SO and a GO. The presented results demonstrate the strong performance of the developed algorithms, both of which aim to enhance the correlation between measured and simulated strain responses. Nevertheless, the GO exhibits superior performance, as it enables a lower variation in material properties within their permissible ranges.

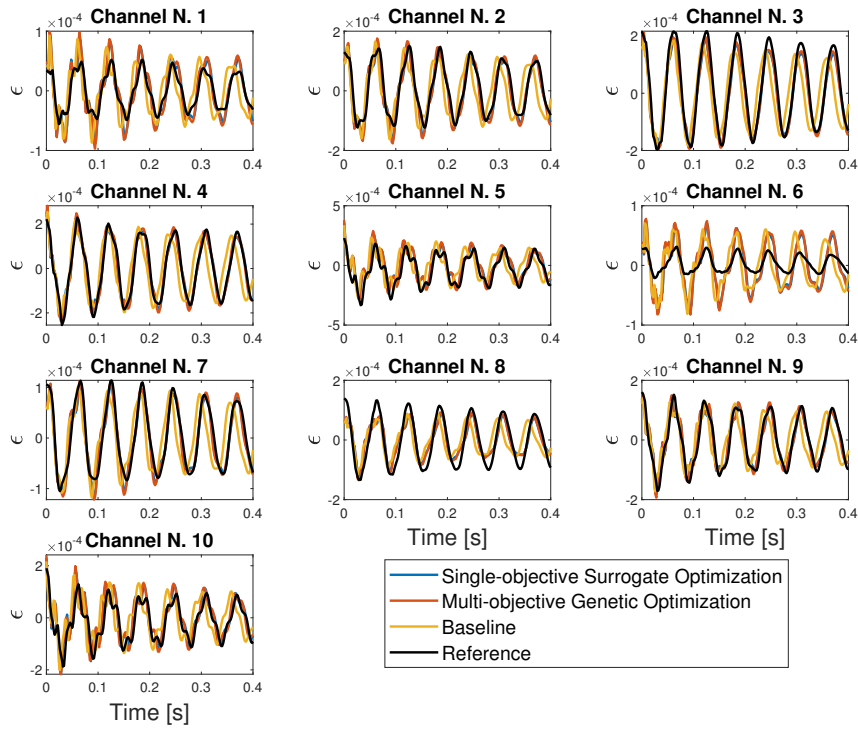


**Figure 5:** Small-scale WT blade: test and simulated strain signals (baseline and updated FEMs)

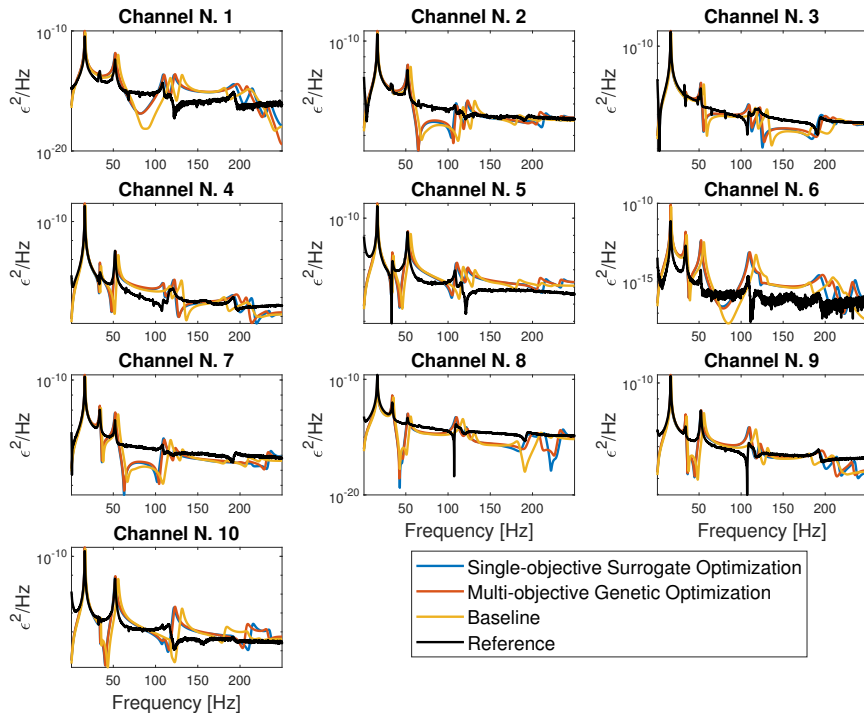


**Figure 6:** Small-scale WT blade: test and simulated strain signals PSDs (baseline and updated FEMs)

## ACKNOWLEDGMENTS

The authors gratefully acknowledge Sentea N.V. for their support in the experimental campaign. The authors would like to also acknowledge DTU and the project “RELIABLADE: Improving Blade Reliability through Application of Digital Twins over Entire Life Cycle”, supported by the Danish Energy Agency through the Energy Technology Development and Demonstration Program (EUDP), Grant No. 64018-0068, the support of which is greatly appreciated.

## REFERENCES

- [1] Amrit Shankar Verma, Nils Petter Vedvik, Philipp Ulrich Haselbach, Zhen Gao, and Zhiyu Jiang. Comparison of numerical modelling techniques for impact investigation on a wind turbine blade. *Composite Structures*, 209:856–878, 2019.
- [2] M. M. Luczak, B. Peeters, S. Manzato, E. Di Lorenzo, K. Reck-Nielsen, P. Berring, P. U. Haselbach, and K. Branner. Research sized wind turbine blade modal tests: Comparison of the impact excitation with shaker excitation. In *Journal of Physics: Conference Series*, volume 1102. Institute of Physics Publishing, 10 2018. doi: 10.1088/1742-6596/1102/1/012022.
- [3] E. Di Lorenzo, S. Manzato, B. Peeters, V. Ruffini, P. Berring, P. U. Haselbach, K. Branner, and M. M. Luczak. Modal analysis of wind turbine blades with different test setup configurations. In *Conference Proceedings of the Society for Experimental Mechanics Series*, pages 143–152. Springer New York LLC, 2020. ISBN 9783030126834. doi: 10.1007/978-3-030-12684-1\_14.
- [4] Fábio Luis Marques dos Santos, Bart Peeters, Marco Menchicchi, Jenny Lau, Ludo Gielen, Wim Desmet, and Luiz Carlos Sandoval Góes. Strain-based dynamic measurements and modal testing. In *Topics in Modal Analysis II, Volume 8: Proceedings of the 32nd IMAC, A Conference and Exposition on Structural Dynamics, 2014*, pages 233–242. Springer, 2014.
- [5] Fábio Luis Marques dos Santos and Bart Peeters. On the use of strain sensor technologies for strain modal analysis: Case studies in aeronautical applications. *Review of Scientific Instruments*, 87(10), 2016.
- [6] E. Coppotelli G. Lampani L. Pasquali-M. Sbarra, R.G. Del Priore. On the use of fiber optic sensors and operational modal analysis for structural health monitoring in aerospace structures. In *Proceedings of ISMA 2024 - International Conference on Noise and Vibration Engineering and USD 2024 - International Conference on Uncertainty in Structural Dynamics*, 2024.
- [7] Lars Glavind, Ib Svend Olesen, Bjarne Funch Skipper, and Martin Kristensen. Fiber-optical grating sensors for wind turbine blades: a review. *Optical Engineering*, 52(3):030901–030901, 2013.
- [8] Rommel G Regis and Christine A Shoemaker. A stochastic radial basis function method for the global optimization of expensive functions. *INFORMS Journal on Computing*, 19(4):497–509, 2007.
- [9] César Pérez López and César Pérez López. Optimization techniques via the optimization toolbox. *MATLAB optimization techniques*, pages 85–108, 2014.
- [10] Silvia Vettori, Emilio Di Lorenzo, Bart Peeters, and Eleni Chatzi. Assessment of alternative covariance functions for joint input-state estimation via gaussian process latent force models in structural dynamics. *Mechanical Systems and Signal Processing*, 213:111303, 2024.
- [11] Kalyanmoy Deb. Multi-objective optimisation using evolutionary algorithms: an introduction. In *Multi-objective evolutionary optimisation for product design and manufacturing*, pages 3–34. Springer, 2011.
- [12] Kalyanmoy Deb, Amrit Pratap, Sameer Agarwal, and TAMT Meyarivan. A fast and elitist multiobjective genetic algorithm: Nsga-ii. *IEEE transactions on evolutionary computation*, 6(2):182–197, 2002.